**Smart Structures and Systems**, *Vol. 27, No. 6 (2021) 917-926*
DOI: https://doi.org/10.12989/sss.2021.27.6.917


# Smart structural stability and NN based intelligent control for nonlinear systems

Tim Chen [1a], Y.C. Huang [2], C.C. Hung [3], Suzanne Frias [2], J.A. Muḥammad [4] and C.Y.J. Chen[*5a]

[1] *Faculty of Information Technology, Ton Duc Thang University, Ho Chi Minh City, Vietnam*
[2] *Department of Earth Science, National Taiwan Normal University, Taipei, Taiwan;*
*Center of Natural Science, Kaohsiung Municipal Fushan Junior High School, Kaohsiung, Taiwan*
[3] *Department of Mechanical Engineering, National Taiwan University, No. 1, Sec. 4, Roosevelt Road, Taipei 10617, Taiwan;*
*Faculty of Electronic Engineering, Taipei Municipal Muzha Vocational High School, 77 Sec. 4 Muzha Rd. Taipei 11656, Taiwan*
[4] *National Physical Laboratory, New Delhi, Dr KS Krishnan Marg, Pusa, New Delhi, Delhi 110012, India*
[5] *Faculty of Engineering, King Abdulaziz University, Jeddah 21589, Saudi Arabia*

(*Received July 14, 2019, Revised November 7, 2020, Accepted March 27, 2021*)

**Abstract.** This paper has proposed an intelligent Evolutionary Bat Algorithm (afterward, EBA) Fuzzy NN (Neural Network) controller used to ensure the asymptotic simulation stability of a mathematics nonlinear system for a smart structure. The smart evolutionary fuzzy NN model adopts an NN numerical model and the linear differential inclusion (LDI) concept. Denotation of the nonlinear dynamics is constructed by transforming the nonlinear model into a multi-rule-based sector nonlinear form of mathematics linear numerical models, and implementing a new sufficient mathematics condition whereby the asymptotic simulation stability of the intelligent structure is guaranteed by the Lyapunov mathematics function, linear matrix inequality (LMI). The high frequency is also injected as an auxiliary to stabilize these nonlinear systems. According to the relaxed method injected with dithered auxiliary, the nonlinear system can be guaranteed stable by appropriately regulating the parameters. Finally, there is a numerical resultant example with simulation results which is designated in order to precisely demonstrate the advantages of the smart intelligent controller and the proposed control scheme compared to previous schemes.

**Keywords:** artificial intelligence; LMI; smart stability; automated design; nonlinear fuzzy control

## 1. Introduction

The most general and useful method for investigating the stability of nonlinear simulation systems is the theory proposed by the Russian mathematician Lyapunov in the late 19th century (Gutman 1979). A report published by Lyapunov in 1892 included two mathematics methods of stability analysis (lined method and direct method). The direct method determines this stability of the nonlinear simulation systems via constructing the scaled energy mathematics function of the simulation system and controlling the time change of the simulation system. Since then, many improvements have been made to the Lyapunov method. Today, Lyapunov's lining method is now the theoretical basis of linear control, and Lyapunov's theory is the most important tool for analyzing and designing non-linear simulation systems. Lyapunov's theory of stability is the lined method and the direct method combined.

A number of nonlinear control mathematics methods for nonlinear simulation systems had been developed and proposed to solve the challenges of controller design in a real simulation system. However, these nonlinear control schemes are too complex to be suitable for practical applications (Chen *et al*. 1999, 2019a, b, 2020, Bedirhanoglu 2014, Zhang 2015). Because the quality of the controller is not seen linearly, direct feedback is difficult to do, so it is certainly not easy to design the simulation system controller for nonlinear simulation systems.

To successfully design these nonlinear simulation system controls, a simplified numerical model for the controller must be developed. In previous research, a fuzzy Takagi-Sugeno (TS) model was modeling practical plants make controller stabilize these fuzzy TS models. However, assuming that the fuzzy model is directly compatible with the nonlinear simulation system, these mathematics methods ignore modeling errors, which can lead to instability. Tanaka and Sugeno (1992), Chen *et al*. (1999, 2020) and Kirakidis (1998) have presented mathematics methods to overcome this instability.

In recent years, the field has developed new mathematics methods, each with unique advantages of solving complex mathematics nonlinear simulation systems, identification and those control mathematics problems (see Shariatmadar and Razavi 2014, Braz-Cesar and Barros 2018, Ghaffarzadeh and Aghabalaei 2017, Pozo *et al*. 2016, Ying *et al*. 2019, Jeong *et al*. 2019, Chen 2014a, b, Son *et al*. 2016, Zhou *et al*. 2015, Tanaka and Sugeno 1992 and its references). Neurons type element for parallel operation of a neural network was design to stimulate the biological nervous simulation system. By adjusting the weights between elements, these NNs can be formed to represent

*Corresponding author, Ph.D.,
E-mail: jc343965@gmail.com
[a] E-mail: timchen@tdtu.edu.vn



ISSN: 1738-1584 (Print), 1738-1991 (Online)

specific mathematics functions. Thus, by repeated learning, the nonlinear numerical simulation system can be approximated to the NN model. However, the stability of the intelligent structure of nonlinear simulation systems is difficult to analyze based on the control of the neural network model and there are few research reports. Therefore, this research uses LDI approach to solve the problem of stability analysis of the intelligent structure of the nonlinear simulation system.

In order to solve the influence of modeling errors, a solid fuzzy mathematics control design scheme based on a neural network is proposed. First, we construct an NN multilayer perceptron, which has an original S-type symmetric transfer mathematics function to approximate nonlinear plants. The numerical dynamics of these NN models are then changed to LDI representation. The numerical model-based simulation fuzzy mathematics controllers are then synthesized simulation in order to numerically stabilize the mathematics nonlinear simulation system. An evolutionary algorithm is proposed to achieve the purpose of modeling the control simulation system. The so-called evolutionary bat algorithm (EBA) is able to solve different types of optimization problems and is thus often incorporated in the design of LDI controllers. Based on the assumption of the Lyapunov stability, a flexible model of structural simulation systems for artificial LDI representation including the stability criterion, for smart structural stability is constructed. Furthermore, fuzzy theory and EBA are considered in the control scheme which make the simulation system control more robust and easier to implement. The rest of the paper on, the design of the intelligent control methodology is organized in the present study as follows. The simulation system is described in the second section. In the case of modeling errors, a common indication is provided which is sufficient for the nonlinear simulation system to ensure the asymptotic simulation stability of the intelligent structure in section three. In Section four, we develop sensitive criteria for structural stability. In section five, we propose the design algorithm. A numerical example with simulation to precisely illustrate these feasibilities of our method is provided in section six, and a summary is designated at the end of this section.

## 2. System simulation description

Consider a numerical and discrete-time mathematics nonlinear simulation system that describes states as

$$\boldsymbol{x}(k+1) = f(\boldsymbol{x}(k), \boldsymbol{u}(k)) \tag{1}$$

in which $f(\cdot)$is a mathematics nonlinear numerical vector-value mathematics function, $x(k)\sim x(k-m+1)$ is the m-dimensional state numerical vector and $u(k)\sim u(k-n+1)$ is the n-dimensional mathematics output numerical vector.

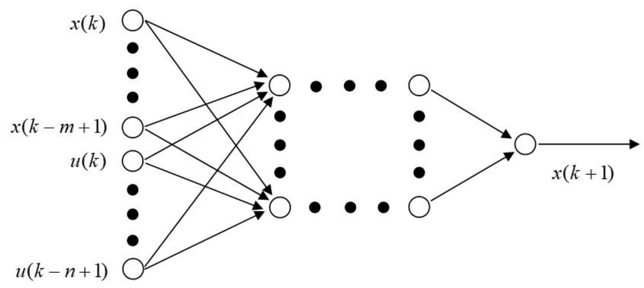


Fig. 1 NN model

Fig. 1 consider an NN model, with $S$ layers and $R^q$ neurons for each of the layer, where the unit $q = 1, 2, \cdots, S$. It could be observed $T(v) \equiv \lambda\{2/[1 + exp\ (-v/\eta)] - 1\}$ $(\eta > 0, \lambda > 0)$ of some units in the NN numerical model. The numerical sigmoid mathematics function with two parameters $\eta$ and $\lambda$ has generalized concept compared with the special case of one parameter sigmoid mathematics function. The weight unit matrix of these $q$th layers are written as $\boldsymbol{W}^q \equiv [T_1(v)\quad T_2(v)\quad \cdots\quad T_{R^q}(v)]^T$, and $T_r$ are the transfer mathematics function numerical vector with $\boldsymbol{\Psi}^q$. Also

$$r = 1, 2, \cdots, R^q \tag{2}$$

The final mathematics output of the numerical NN model could be referred in the follows

$$x(k+1) = \boldsymbol{\Psi}^S\left(\boldsymbol{W}^S \times \boldsymbol{\Psi}^{S-1}\left(\boldsymbol{W}^{S-1} \times \boldsymbol{\Psi}^{S-2}\left(\cdots\cdots \boldsymbol{\Psi}^2\left(\boldsymbol{W}^2 \times \boldsymbol{\Psi}^1\big(\boldsymbol{W}^1 \times \boldsymbol{Z}(k)\big)\right)\cdots\cdots\right)\right)\right) \tag{3}$$

$$\boldsymbol{Z}(k)^T = [x(k)\quad \cdots\quad x(k-m+1)\quad u(k)\quad \cdots\quad u(k-n+1)]. \tag{4}$$

Accordingly, LDI is introduced into the state spatial representation, which is (Tanaka 1995, Tsai and Chen 2014)

$$\begin{gathered}\boldsymbol{y}(k+1) = D\big(\boldsymbol{a}(k)\big)\boldsymbol{y}(k)\\ D\big(\boldsymbol{a}(k)\big) = \sum_{i=1}^{\varphi} h_i\big(\boldsymbol{a}(k)\big)D_i,\end{gathered} \tag{5}$$

where $\varphi$ is kind of a positive numerical integer, unit $\boldsymbol{a}(k)$ is a numerical vector which signify these dependences of $h_i(\cdot)$. In terms of LDI characteristics, without losing generality, some can employ $h_i(k)$ instead of unit $h_i(\boldsymbol{a}(k))$. Firstly, it can be obviously found that $T(v)$ is satisfying $g_1 v \le T(v) \le g_2 v,\ v \ge 0$ and $g_2 v \le T(v) \le g_1 v,\ v < 0$.

The transfer numerical mathematics function numerical vector unit $\boldsymbol{\Psi}^q$ and net mathematics output numerical vector unit $v^q$, the min-max numerical matrix $\boldsymbol{G}(v^q, \boldsymbol{\Psi}^q)$ is then defined as the following

$$\boldsymbol{G}(v^q, \boldsymbol{\Psi}^q) \equiv diag\big(g(T_r)\big), \qquad r = 1, 2, \cdots, R^q. \tag{6}$$

Furthermore, based on these interpolation mathematics methods and the Eq. (4), we acquire

$$x(k+1)=\{\sum_{j_1^S=1}^{2}\cdots\sum_{j_{R^S}^S=1}^{2}h_{j_1^S}^S(k)\cdots h_{j_{R^S}^S}^S(k)\boldsymbol{G}(v^S,\boldsymbol{\Psi}^S)\,(\boldsymbol{W}^S\times[\cdots\cdots[\sum_{j_1^2=1}^{2}\cdots\sum_{j_{R^2}^2=1}^{2}h_{j_1^2}^2(k)\cdots h_{j_{R^2}^2}^2(k) \tag{7}$$

$$\cdot\,\boldsymbol{G}(v^2,\boldsymbol{\Psi}^2)(\boldsymbol{W}^2\times\left[\sum_{j_1^1=1}^{2}\cdots\sum_{j_{R^1}^1=1}^{2}h_{j_1^1}^1(k)\cdots h_{j_{R^1}^1}^1(k)\boldsymbol{G}(v^1,\boldsymbol{\Psi}^1)\,(\boldsymbol{W}^1\times\boldsymbol{Z}(k))]\right])]\cdots\cdots])\}=\sum_{v}h_v(k)\boldsymbol{J}_v(\boldsymbol{W},\boldsymbol{\Psi})\boldsymbol{Z}(k) \tag{8}$$

where

$$h_1^q(k),\quad h_2^q(k)\in[0,\quad 1],$$
$$\sum_{j_r^q=1}^{2}h_{j_r^q}^q(k)=1,$$
$$\sum_{v^q}h_{v^q}^q(k)=\sum_{j_1^q=1}^{2}\cdots\sum_{j_{R^q}^q=1}^{2}h_{j_1^q}^q(k)\cdots h_{j_{R^q}^q}^q(k),$$
$$\boldsymbol{J}_v\equiv\boldsymbol{G}(v^S,\boldsymbol{\Psi}^S)\boldsymbol{W}^S\cdots\boldsymbol{G}(v^1,\boldsymbol{\Psi}^1)\boldsymbol{W}^1,$$
$$h_v(k)>0,$$
$$\sum_{v}h_v(k)\equiv\sum_{v^S}\cdots\sum_{v^1}h_{v^S}^S(k)\cdots h_{v^1}^1(k)=1.$$

The dynamics of the NN numerical model Eq. (8) could then be numerically rewritten as follows with LDI representation

$$\begin{aligned}\boldsymbol{x}(k+1)&=\sum_{i=1}^{\varphi}h_i(k)\boldsymbol{J}_i\boldsymbol{Z}(k)\\&=\sum_{i=1}^{\varphi}h_i(k)\{\boldsymbol{A}_i\boldsymbol{x}(k)+\boldsymbol{B}_i\boldsymbol{u}(k)\}\end{aligned} \tag{9}$$

where

$\boldsymbol{x}(k)^T=[x(k)\quad x(k-1)\quad\cdots\quad x(k-m+1)]$, $\boldsymbol{u}(k)^T=[u(k)\quad u(k-1)\quad\cdots\quad u(k-n+1)]$, and $\boldsymbol{J}_i$ is the appropriate dimension which is associated with $\boldsymbol{J}_v(\boldsymbol{W},\boldsymbol{\Psi})$. Besides, units $\boldsymbol{A}_i$ and $\boldsymbol{B}_i$ are respectively the partitions of unit $\boldsymbol{J}_i$ which is corresponding to the mathematics partition $\boldsymbol{Z}(k)^T=[x(k)\quad\cdots\quad x(k-m+1)\quad u(k)\quad\cdots\quad u(k-n+1)]$.

Herein, the synthesized fuzzy controllers are in the form of

$$\begin{aligned}&\text{IF } x_1(k) \text{ is } M_{i1} \text{ and } \cdots \text{ and } x_m(k) \text{ is } M_{im}\\&\text{THEN}\quad \boldsymbol{u}(k)=\boldsymbol{K}_i\boldsymbol{x}(k),\quad i=1,2,\cdots,\mu\end{aligned} \tag{10}$$

where $\mu$ is the numerical number of IF-THEN logic rules and the last mathematics output of these numerical controller is then referred in the following

$$\boldsymbol{u}(k)=\frac{\sum_{i=1}^{\mu}w_i(k)\boldsymbol{K}_i\boldsymbol{x}(k)}{\sum_{i=1}^{\mu}w_i(k)}=\sum_{i=1}^{\mu}\hat{h}_i(k)\boldsymbol{K}_i\boldsymbol{x}(k) \tag{11}$$

with

$$w_i(k)=\prod_{j=1}^{m}M_{ij}\left(x_j(k)\right),\qquad \hat{h}_i(k)=\frac{w_i(k)}{\sum_{i=1}^{\mu}w_i(k)}$$

in which $M_{ij}(x_j(k))$ is these grades in membership of unit $x_j(k)$ in $M_{ij}$. In these studies, they are also assumed in the form of unit $w_i(k)\geq 0$, and $\sum_{i=1}^{\mu}w_i(k)>0$ for all kinds of $k$. Therefore, the unit $\hat{h}_i(k)\geq 0$, $i=1,2,\cdots,\mu$ and $\sum_{i=1}^{\mu}\hat{h}_i(k)=1$ for these units $k$.

## 3. Fuzzy robustness smart control design

In this section, the mathematics nonlinear closed-loop smart structural asymptotically stable simulation system is evaluated and considered under these influences of numerical modeling error $\boldsymbol{e}(k)$. The issue of modeling error is presented and ensured for smart structural asymptotic and associated stability of the numerical nonlinear simulation system derived below.

If substituting Eq. (11) into Eq. (1), which yields these closed-loop mathematics nonlinear simulation systems as follows

$$\begin{aligned}&\boldsymbol{x}(k+1)\\&=\sum_{i=1}^{\varphi}\sum_{j=1}^{\mu}h_i(k)\hat{h}_j(k)\big(\boldsymbol{A}_i+\boldsymbol{B}_i\boldsymbol{K}_j\big)\boldsymbol{x}(k)+\{F(\boldsymbol{x}(k))\\&-\sum_{i=1}^{\varphi}\sum_{j=1}^{\mu}h_i(k)\hat{h}_j(k)\big(\boldsymbol{A}_i+\boldsymbol{B}_i\boldsymbol{K}_j\big)\boldsymbol{x}(k)\}\\&=\sum_{i=1}^{\varphi}\sum_{j=1}^{\mu}h_i(k)\hat{h}_j(k)\boldsymbol{H}_{ij}\boldsymbol{x}(k)+\boldsymbol{e}(k)\end{aligned} \tag{12}$$

where

$$F(\boldsymbol{x}(k))\equiv f(\boldsymbol{x}(k),\boldsymbol{u}(k)),\quad \boldsymbol{H}_{ij}=\boldsymbol{A}_i+\boldsymbol{B}_i\boldsymbol{K}_j,$$
$$\boldsymbol{e}(k)=\left\{F(\boldsymbol{x}(k))-\sum_{i=1}^{\varphi}\sum_{j=1}^{\mu}h_i(k)\,\hat{h}_j(k)\big(\boldsymbol{A}_i+\boldsymbol{B}_i\boldsymbol{K}_j\big)\,\boldsymbol{x}(k)\right\} \tag{13}$$

and supposing the fact that there exits a bounding numerical matrix $\Delta\boldsymbol{H}_{ij}$, for example

$$\|\,\boldsymbol{e}(k)\,\|\leq\left\|\sum_{i=1}^{\varphi}\sum_{j=1}^{\mu}h_i(k)\hat{h}_j(k)\Delta\boldsymbol{H}_{ij}\boldsymbol{x}(k)\right\| \tag{14}$$

$$\Delta\boldsymbol{H}_{ij}=\delta_{ij}\boldsymbol{H}_q \tag{15}$$

We could derive

$$(k)^T\boldsymbol{e}(k)\leq\{\boldsymbol{H}_q\boldsymbol{x}(k)\}^T\{\boldsymbol{H}_q\boldsymbol{x}(k)\} \tag{16}$$

which demonstrates the modeling error in Eq. (13) is bounded particularly by the specified $\boldsymbol{H}_q$.

Herein, an important criterion is then designated as below to basically guarantee these Smart Structural asymptotic stabilities of these closed-loop numerical nonlinear simulation system Eq. (12).

**Theorem 3.1**:

If there exist a numerically positive definite matrix $P$ and then there is a positive changeable constant unit $\kappa$ and result in that the following inequality

$$\left(\frac{\boldsymbol{H}_{ij}+\boldsymbol{H}_{ji}}{2}\right)^T \boldsymbol{P}\left(\frac{\boldsymbol{H}_{ij}+\boldsymbol{H}_{ji}}{2}\right)-\boldsymbol{P}+\left(\kappa\, \boldsymbol{H}_{ij}^T\boldsymbol{P}\boldsymbol{H}_{ij}\right) +(1+\kappa^{-1})\lambda_M(\boldsymbol{P})\boldsymbol{H}_q^T\boldsymbol{H}_q]\boldsymbol{x}(k)<0 \tag{17}$$

is satisfied for the parameters$i=1,2,\cdots,\varphi;\ j=1,2,\cdots,\mu$ where unit $\lambda_M(\boldsymbol{P})$ means the numerical maximum eigenvalue of unit $\boldsymbol{P}$, then these closed-loop numerical nonlinear simulation systems Eq. (12) is then asymptotically stable.

Based on the learning from bats in the natural world, the EBA is discussed (Tsai *et al.* 2015). Unlike other swarm information algorithms, the advantage of EBA is only in case that one parameter (called the medium) calls for need to be determined and then these algorithms are used to solve the problem. In the process of evolution, the choice of different medium will determine the different stages of the research. In this study, we chose air in the reason that these original media we introduced in the natural and physical environment in which bats basically live. These operations of EBA could be simplified in four stages:

Origin: randomly assign artificial reactions to them, and disperse them in the solution space.

Movement: Say the artificial preparation is moved. Create a random mathematics number, then check if it exceeds the fixed pulse mathematics emission rate. Upon the result is positive, use a random walking process to move the artificial preparation.

$$x_i^t = x_i^{t-1}+D,$$

In which $x_i^t$ demonstrates the unit coordinate of these $i$-th artificial mathematics agents at the $t$-th iteration, unit $x_i^{t-1}$ demonstrates the possible mathematics coordinate of these $i$-th artificial mathematics agents at the ending iteration, and unit $D$ is the numerical moving mathematics distance that these artificial mathematics agents go to these iterations.

$$D=\gamma\cdot\Delta T$$

In which unit $\gamma$ is a numerical constant which is corresponding to these possible mediums which was chosen for these numerical experiments.

$$x_i^{t_R}=\beta(x_{best}-x_i^t),\quad \beta\in[0,1]$$

In which $\beta$ is a numerical random number; unit $x_{best}$ represents the coordinate of these near and best solutions which are found so far all throughout all of those artificial mathematics agents, and unit $x_i^{t_R}$ denotes the new numerical coordinates of these artificial mathematics agents after these operations of the numerical random all walk in the process.

## 4. Smart NN relaxed simulation system and the stability analyses

In the section, a smart structural stability criterion is presented to stabilize the numerical simulation system utilizing the same fuzzy controller designed.

The corresponding relaxed simulation system Eq. (18) is defined as

$$\boldsymbol{x}_R(k+1)=\sum_{m=1}^{\tau}\alpha_m(k)\,f(\boldsymbol{x}_R(k),\boldsymbol{u}_R(k),\beta_m(k)) \tag{18}$$

where $\alpha_m(k)$ is regarded with non-negative and it satisfies

$$0\le\alpha_m(k)\le 1,\quad \sum_{m=1}^{\tau}\alpha_m(k)=1 \tag{19}$$

In the subsection, the NN numerical model of the relaxed simulation system (will be called as "NN relaxed simulation system" in the following text) is reconstructed. First, the last mathematics output of these closed-loop NN relaxed simulation systems are describing as follows in the form of

$$x(k+1)=\sum_v \bar{h}_v(k)\bar{\boldsymbol{J}}_v(\bar{\boldsymbol{W}},\boldsymbol{\Psi})\boldsymbol{Z}(k) \tag{20}$$

where

$$\bar{\boldsymbol{J}}_v\equiv\boldsymbol{G}(v^S,\boldsymbol{\Psi}^S)\bar{\boldsymbol{W}}^S\cdots\boldsymbol{G}(v^1,\boldsymbol{\Psi}^1)\bar{\boldsymbol{W}}^1,$$
$$\bar{h}_v(k)>0,\quad \sum_v\bar{h}_v(k)=1$$

Then, the same fuzzy controller synthesized in Eq. (11) is used to stabilize the numerical simulation system. Next, the numerical dynamics of these NN relaxed models are rewritten as the LDI representation with $\bar{h}_i(k)\ge 0$, $\sum_{i=1}^{\varphi}\bar{h}_i(k)=1$

$$\boldsymbol{x}(k+1)=\sum_{i=1}^{\varphi}\sum_{j=1}^{\mu}\bar{h}_i(k)\hat{h}_j(k)\{\bar{\boldsymbol{A}}_i(\alpha_m,\beta_m)+\bar{\boldsymbol{B}}_i(\alpha_m,\beta_m)\boldsymbol{K}_j\}\boldsymbol{x}(k) \tag{21}$$

In the remainder of this study, we replace $\bar{\boldsymbol{A}}_i(\alpha_m,\beta_m)$ and $\bar{\boldsymbol{B}}_i(\alpha_m,\beta_m)$ with $\bar{\boldsymbol{A}}_i$ and $\bar{\boldsymbol{B}}_i$, respectively. Hence, some could appropriately calculate and regulate these parameters $\alpha_m$ and $\beta_m$ to get the appropriate matrices $\bar{\boldsymbol{A}}_i$ and $\bar{\boldsymbol{B}}_i$. According to Eq. (12) some have the numerical closed-loop simulation system in the following

$$\boldsymbol{x}(k+1)=\sum_{i=1}^{\varphi}\sum_{j=1}^{\mu}\bar{h}_i(k)\hat{h}_j(k)\bar{\boldsymbol{H}}_{ij}\boldsymbol{x}(k)+\bar{\boldsymbol{e}}(k) \tag{22}$$

where

$$
\begin{aligned}
&F\big(\boldsymbol{x}(k), d(k)\big) \equiv f\big(\boldsymbol{x}(k), \boldsymbol{u}(k), d(k)\big),\\
&\bar{\boldsymbol{H}}_{ij} = \bar{\boldsymbol{A}}_i + \bar{\boldsymbol{B}}_i \boldsymbol{K}_j,\\
&\bar{\boldsymbol{e}}(k) = \{F(\boldsymbol{x}(k), d(k))\\
&\qquad - \sum_{i=1}^{\varphi}\sum_{j=1}^{\mu} \bar{h}_i(k)\,\hat{h}_j(k)\big(\bar{\boldsymbol{A}}_i + \bar{\boldsymbol{B}}_i \boldsymbol{K}_j\big)\,\boldsymbol{x}(k)\}
\end{aligned} \tag{23}
$$

In similar fashion, suppose the results that there exits a bounding numerical matrix $\Delta\bar{\boldsymbol{H}}_{ij}$ such resulted from

$$
\| \bar{\boldsymbol{e}}(k) \| \le \left\| \sum_{i=1}^{\varphi}\sum_{j=1}^{\mu} \bar{h}_i(k)\hat{h}_j(k)\Delta\bar{\boldsymbol{H}}_{ij}\boldsymbol{x}(k) \right\| \tag{24}
$$

$$
\Delta\bar{\boldsymbol{H}}_{ij} = \delta_{ij}\bar{\boldsymbol{H}}_q \tag{25}
$$

where $\|\delta_{ij}\| \le 1$, for $i = 1, 2, \cdots, \varphi$ and $j = 1, 2, \cdots, \mu$.

Herein, a smart structural stability criterion with the parameters is designated below to precisely guarantee the smart structural asymptotic simulation stability of the numerical closed-loop simulation system Eq. (22).

**Theorem 4.1**

The numerical closed-loop simulation system is asymptotically and precisely stable if there is existing a positive definite numerical matrix $\boldsymbol{Q}$ and a positive constant value $\kappa$ resulting in the following inequality

$$
\begin{aligned}
&\left(\frac{\bar{\boldsymbol{H}}_{ij} + \bar{\boldsymbol{H}}_{ji}}{2}\right)^T \boldsymbol{Q} \left(\frac{\bar{\boldsymbol{H}}_{ij} + \bar{\boldsymbol{H}}_{ji}}{2}\right) - \boldsymbol{Q} + \big(\kappa\, \bar{\boldsymbol{H}}_{ij}^T \boldsymbol{Q} \bar{\boldsymbol{H}}_{ij}\big)\\
&+(1+\kappa^{-1})\lambda_M(\boldsymbol{Q})\bar{\boldsymbol{H}}_q^T\bar{\boldsymbol{H}}_q]\boldsymbol{x}(k) < 0
\end{aligned} \tag{26}
$$

is satisfied for $i = 1, 2, \cdots, \varphi$; $j = 1, 2, \cdots, \mu$ where $\lambda_M(\boldsymbol{Q})$ represents the maximum numerical eigenvalue of $\boldsymbol{Q}$.

The solid proof of these Theorem could be discussed in the same way by the follows in these same procedures while these proofs of Theorem 3.1, but with $\boldsymbol{H}_{ij}$ being replaced by $\bar{\boldsymbol{H}}_{ij}$. Therefore, this proof is not repeated here.

## 5. Derived algorithm

The whole design process can be precisely summarized to synthesize a model based smart fuzzy controller with the following steps.

Step no. 1: Establish an NN numerical model, then convert it to LDI formulation.

Step no. 2: Synthesize a model-based fuzzy controller.

Step no. 3: Select the bounding matrix $\Delta\boldsymbol{H}_{ij} (= \delta_{ij}\boldsymbol{H}_q)$ to satisfy robustness design.

Step no. 4: If there exists a numerically positive definite numerical $\boldsymbol{P}$ to satisfy these stability simulation conditions Eq. (17), the simulation system could be precisely stabilized by these synthesized controllers.

Step no. 5: Apply the EBA relaxed method to establish the relaxed simulation system.

Step 6: Reconstruct an EBA NN model of the relaxed simulation system and then convert it into LDI representation.

Step no. 7: Select the bounding matrix $\Delta\bar{\boldsymbol{H}}_{ij}$ $(= \delta_{ij}\bar{\boldsymbol{H}}_q)$ to satisfy robustness design.

Step no. 8: Adjust the parameters $\alpha_m$ and $\beta_m$ to satisfy the stability condition Eq. (26).

## 6. Example

Consider a mode control of seismically excited structures by the following equation (Tanaka 1995)

$$
x(k+1) = -1.1x(k-1) + 0.2x(k)^2u(k). \tag{27}
$$

It can be easily seen that at least near the starting point, the powerless simulation system is unstable. These purposes of the examples are to synthesize a model-based EBA fuzzy numerical controller for this mathematics nonlinear simulation system.

Step 1: A simulation appropriate NN numerical model which is shown in Fig. 2 with two simulation layers in which the hidden simulation layer makes of two fuzzy neurons and these mathematics output layers are used to approximate nearly the mathematics nonlinear numerical simulation system Eq. (27). After our training the neurons by the introducing backpropagation algorithm, the unit weights could be designated as the following results (The training process can be referred in manual book of Matlab toolbox and the detail is not repeated here. Also, we use as few as layers and hidden neurons to show the robustness of the proposed criterion)

$$
\begin{aligned}
&W_{11}^1 = 0.4164, \quad W_{12}^1 = 0.3997, \quad W_{13}^1 = -0.1423,\\
&W_{21}^1 = -0.5647, \quad W_{22}^1 = -0.2601, \quad W_{23}^1 = 0.1626,\\
&W_{31}^1 = -8.9071, \quad W_{32}^1 = -7.0720.
\end{aligned}
$$

From Fig. 2 we have†

$$
\begin{aligned}
&v_r^1 = W_{r1}^1 x(k) + W_{r2}^1 x(k-1) + W_{r3}^1 u(k),\\
&r = 1, 2
\end{aligned} \tag{28}
$$

$$
v_1^2 = W_{11}^2\, T(v_1^1) + W_{12}^2\, T(v_2^1) \tag{29}
$$

$$
x(k+1) = T(v_1^2) \tag{30}
$$

where

$$
T(v_r^1) = \frac{2}{\left[1 + exp\ \left(-\frac{v_r^1}{0.5}\right)\right]} - 1, \qquad r = 1, 2 \tag{31}
$$

$$
T(v_1^2) = 2/\left[1 + exp\ \left(-\frac{v_r^2}{0.5}\right)\right] - 1. \tag{32}
$$

According to Eqs. (31)-(32), the minimum numerical value and the mathematics maximum numerical value of the mathematics derivative of unit $\mathrm{T}(v)$ could thus be designated in the following form

† The symbol $v_b^a$ represents the net numerical input of the possible $b$th fuzzy neuron of the $a$th simulation layer.

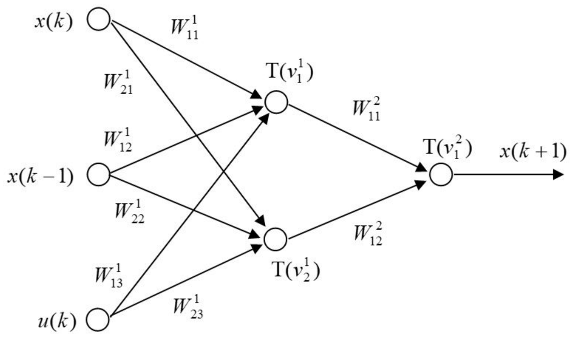


Fig. 2 The NN model of Eq. (27)

$$g_1 = \min_v \frac{d\,T(v)}{d\,v} = 0, \qquad g_2 = \max_v \frac{d\,T(v)}{d\,v} = 1.$$

Nevertheless, according to the interpolation numerical method, the Eqs. (31)-(32) could be denoted in the form of

$$Tv_r^1) = \left(h_{r1}^1(k)g_1 + h_{r2}^1(k)g_2\right)v_r^1, \quad r = 1, 2 \tag{33}$$

$$T(v_1^2) = \left(h_{11}^2(k)g_1 + h_{12}^2(k)g_2\right)v_1^2. \tag{34}$$

From Eqs. (30) and (34), we get

$$\begin{aligned} x(k+1) &= \left(h_{11}^2(k)g_1 + h_{12}^2(k)g_2\right)v_1^2 \\ &= \sum_{k=1}^{2} h_{1l}^2(k) g_l v_1^2. \end{aligned} \tag{35}$$

Substituting Eqs. (29), (33)-(34) into Eq. (35) yields

$$\begin{aligned} x(k+1) &= \sum_{l=1}^{2} h_{1l}^2(k) g_l \sum_{r=1}^{2} W_{1r}^2 T(v_r^1) \\ &= \sum_{l=1}^{2} h_{1l}^2(k) g_l \sum_{p=1}^{2}\sum_{s=1}^{2} \begin{matrix} h_{1p}^1(k) h_{2s}^1(k) \\ (g_p W_{11}^2 v_1^1 + g_s W_{12}^2 v_2^1) \end{matrix} \end{aligned} \tag{36}$$

By plugging Eq. (28) into Eq. (36), we obtain

$$\begin{aligned} &x(k+1) \\ &= \sum_{l=1}^{2}\sum_{p=1}^{2}\sum_{s=1}^{2} h_{1l}^2(k) h_{1p}^1(k) h_{2s}^1(k) \{ g_l(g_p W_{11}^2 W_{11}^1 \\ &\qquad + g_s W_{12}^2 W_{21}^1) x(k) + g_l(g_p W_{11}^2 W_{12}^1 \\ &\qquad + g_s W_{12}^2 W_{22}^1) x(k-1) \end{aligned} \tag{37}$$

The matrix representation of Eq. (37) is

$$\boldsymbol{x}(k+1) = \sum_{l=1}^{2}\sum_{p=1}^{2}\sum_{s=1}^{2} \begin{matrix} h_{1l}^2(k) h_{1p}^1(k) h_{2s}^1(k) \\ \left(\boldsymbol{A}_{lps}\boldsymbol{x}(k) + \boldsymbol{B}_{lps} u(k)\right) \end{matrix} \tag{38}$$

where

Moreover, according to renumbering the numerical matrices, the NN numerical model Eq. (38) could be transformed into the proceeding LDI form in representation

$$\boldsymbol{x}(k+1) = \sum_{i=1}^{4} h_i(k)(\boldsymbol{A}_i \boldsymbol{x}(k) + \boldsymbol{B}_i u(k)) \tag{39}$$

In which

$$\begin{aligned} h_1(k) &= h_{11}^2(k)h_{11}^1(k)h_{21}^1(k) + h_{11}^2(k)h_{11}^1(k)h_{22}^1(k) \\ &\quad + h_{11}^2(k)h_{12}^1(k)h_{21}^1(k) + h_{11}^2(k)h_{12}^1(k)h_{22}^1(k) \\ &\quad + h_{12}^2(k)h_{11}^1(k)h_{21}^1(k), \\ h_2(k) &= h_{12}^2(k)h_{11}^1(k)h_{22}^1(k), \\ h_3(k) &= h_{12}^2(k)h_{12}^1(k)h_{21}^1(k), \\ h_4(k) &= h_{12}^2(k)h_{12}^1(k)h_{22}^1(k), \end{aligned}$$

and

$$\begin{aligned} \boldsymbol{A}_1 &= \boldsymbol{A}_{1ps} = \boldsymbol{A}_{211} = \begin{bmatrix} 0 & 0 \\ 1 & 0 \end{bmatrix}, \\ \boldsymbol{A}_2 &= \boldsymbol{A}_{212} = \begin{bmatrix} 3.9933 & 1.8393 \\ 1 & 0 \end{bmatrix}, \\ \boldsymbol{A}_3 &= \boldsymbol{A}_{221} = \begin{bmatrix} -3.7091 & -3.5601 \\ 1 & 0 \end{bmatrix}, \\ \boldsymbol{A}_4 &= \boldsymbol{A}_{222} = \begin{bmatrix} 0.2843 & -1.7208 \\ 1 & 0 \end{bmatrix}, \\ \boldsymbol{B}_1 &= \boldsymbol{B}_{1ps} = \boldsymbol{B}_{211} = \begin{bmatrix} 0 \\ 0 \end{bmatrix}, \qquad p, s = 1, 2, \\ \boldsymbol{B}_2 &= \boldsymbol{B}_{212} = \begin{bmatrix} -1.1501 \\ 0 \end{bmatrix}, \\ \boldsymbol{B}_3 &= \boldsymbol{B}_{221} = \begin{bmatrix} 1.2674 \\ 0 \end{bmatrix}, \\ \boldsymbol{B}_4 &= \boldsymbol{B}_{222} = \begin{bmatrix} 0.1173 \\ 0 \end{bmatrix}. \end{aligned}$$

**Step 2:** The membership mathematics functions of method Rule 1 and method Rule 2 are indicated in Fig. 3 and the fuzzy controllers are basically synthesized in the following form:

Control Rules:

$$\begin{aligned} &\text{IF } x(k) \text{ is } M_1 \text{ THEN unit } u(k) = \boldsymbol{K}_1 \boldsymbol{x}(k), \\ &\text{IF } x(k) \text{ is } M_2 \text{ THEN unit } u(k) = \boldsymbol{K}_2 \boldsymbol{x}(k), \\ &\text{IF unit } x(k) \text{ is } M_3 \text{ THEN } u(k) = \boldsymbol{K}_3 \boldsymbol{x}(k), \\ &\text{IF } x(k) \text{ is } M_4 \text{ THEN } u(k) = \boldsymbol{K}_4 \boldsymbol{x}(k) \end{aligned} \tag{40}$$

where $\boldsymbol{K}_1 = [2 \quad -1]$, $\boldsymbol{K}_2 = [-1 \quad 2]$, $\boldsymbol{K}_3 = [-3 \quad 1]$, $\boldsymbol{K}_4 = [-2 \quad 4]$.

**Steps 3-4:** According to robustness design, an appropriate bounding numerical matrix is thus chosen as

$$\boldsymbol{H}_q = \begin{bmatrix} -3.3801 & -1.0317 \\ 0.45 & 0 \end{bmatrix}, \quad \delta_{ij} = I. \tag{41}$$

Furthermore, the assumption robustness design is thus satisfied from the showing illustration as seen in Fig. 4.

$$\boldsymbol{A}_{lps} = \begin{bmatrix} g_l\left(g_p W_{11}^2 W_{11}^1 + g_s W_{12}^2 W_{21}^1\right) & g_l\left(g_p W_{11}^2 W_{12}^1 + g_s W_{12}^2 W_{22}^1\right) \\ 1 & 0 \end{bmatrix},$$

$$\boldsymbol{B}_{lps} = \begin{bmatrix} g_l\left(g_p W_{11}^2 W_{13}^1 + g_s W_{12}^2 W_{23}^1\right) \\ 0 \end{bmatrix}, \boldsymbol{x}(k)^T = [x(k) \quad x(k-1)].$$

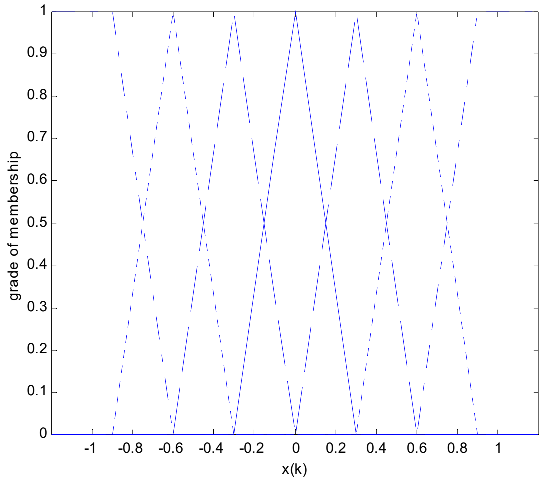


Fig. 3 Membership mathematics functions (Rule 1: 'solid', Rule 2: 'dash', Rule 3: dot', Rule 4: 'dash-dot')

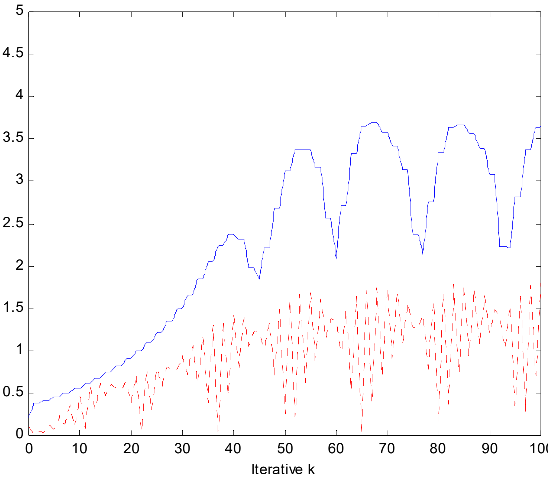


Fig. 4 The plots of $\left\| F\big(\boldsymbol{x}(k), d(k)\big) - \sum_{i=1}^{\varphi}\sum_{j=1}^{\mu} \bar{h}_i(k)\,\hat{h}_j(k)\big(\boldsymbol{A}_i + \boldsymbol{B}_i\boldsymbol{K}_j\big)\,\boldsymbol{x}(k) \right\|$ (dash-dot line) and $\left\| \sum_{i=1}^{\varphi}\sum_{j=1}^{\mu} \bar{h}_i(k)\hat{h}_j(k)\Delta\boldsymbol{H}_{ij}\boldsymbol{x}(k) \right\|$ (solid line)

However, there doesn't exist any positive definite numerical matrix $\boldsymbol{P}$ to basically satisfy the Smart Structural stability condition Eq. (17). The response of $x(k)$ for the simulation closed-loop mathematics nonlinear simulation system is illustrated in Fig. 5. In term of Fig. 5, the mathematics nonlinear numerical simulation system Eq. (27) cannot be asymptotically and precisely stabilized via the introducing synthesized fuzzy controller Eq. (40).

**Step 5:** The mathematics nonlinear simulation system can be written as follows

$$x(k+1) = -1.1x(k-1) + 0.2(d(k) + x(k))^2 u(k). \quad (42)$$

Based on Eq. (19), the corresponding relaxed simulation system of Eq. (42) is established as the showing equation

$$\begin{aligned} x(k+1) = -1.1x(k-1) + 0.2(\alpha_1(\beta_1 + x(k))^2 \\ +\alpha_2(\beta_2 + x(k))^2)u(k) \end{aligned} \quad (43)$$

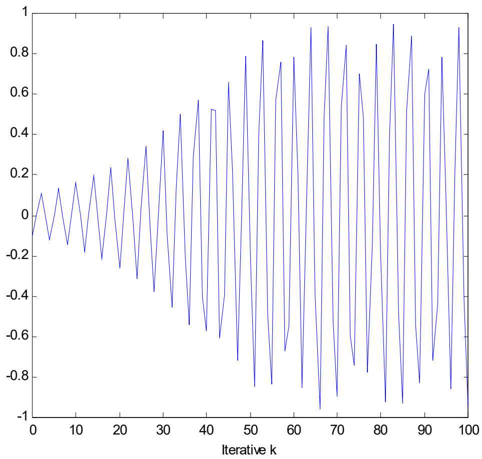


Fig. 5 The response of $x(k)$ for the closed-loop mathematics nonlinear simulation system (unstable)

where $\alpha_i$ and $\beta_i$ are the parameters for $i = 1, 2$. Next, we choose that

$$\alpha_1 = 0.5, \quad \alpha_2 = 1 - \alpha_1 = 0.5 \quad (44)$$

and

$$\beta_1 = -\beta_2 = \xi \quad (45)$$

where $\xi$ is a real constant number. By plugging Eqs. (44)-(45) into Eq. (43), we obtain

$$x(k+1) = -1.1x(k-1) + 0.2(x(k)^2 + \xi^2)u(k). \quad (46)$$

**Step 6:** In the follows, we purpose and find a possibly appropriate amplitude $\xi$ to reasonably stabilize the closed-loop simulation system with the use of EBA fuzzy controller Eq. (40)

By the same procedure as that in Step 1, we have

$$\begin{aligned} v_r^1 &= \bar{W}_{r1}^1(\xi)x(k) + \bar{W}_{r2}^1(\xi)x(k-1) \\ &+\bar{W}_{r3}^1(\xi)u(k), \qquad r = 1, 2 \end{aligned} \quad (47)$$

$$v_1^2 = \bar{W}_{11}^2(\xi)\,T(v_1^1) + \bar{W}_{12}^2(\xi)\,T(v_2^1) \quad (48)$$

$$x(k+1) = \mathrm{T}(v_1^2). \quad (49)$$

According to Eq. (36), we can get

$$\begin{aligned} x(k+1) = \sum_{l=1}^{2}\sum_{p=1}^{2}\sum_{s=1}^{2} \bar{h}_{1l}^2(k)\bar{h}_{1p}^1(k)\bar{h}_{2s}^1(k) \\ \Big\{g_l\Big(g_p\bar{W}_{11}^2(\xi)\bar{W}_{11}^1(\xi) + g_s\bar{W}_{12}^2(\xi)\bar{W}_{21}^1(\xi)\Big)x(k) \\ +g_l\Big(g_p\bar{W}_{11}^2(\xi)\bar{W}_{12}^1(\xi) + g_s\bar{W}_{12}^2(\xi)\bar{W}_{22}^1(\xi)\Big)x(k-1) \\ +g_l\Big(g_p\bar{W}_{11}^2(\xi)\bar{W}_{13}^1(\xi) + g_s\bar{W}_{12}^2(\xi)\bar{W}_{23}^1(\xi)\Big)u(k)\Big\} \end{aligned} \quad (50)$$

The matrix representation of Eq. (50) is

$$\begin{aligned} \boldsymbol{x}(k+1) = \sum_{l=1}^{2}\sum_{p=1}^{2}\sum_{s=1}^{2} \bar{h}_{1l}^2(k)(k)\bar{h}_{1p}^1(k)\bar{h}_{2s}^1(k) \\ (\bar{\boldsymbol{A}}_{lps}\boldsymbol{x}(k) + \bar{\boldsymbol{B}}_{lps}u(k)) \end{aligned} \quad (51)$$

where

$$\bar{\boldsymbol{A}}_{lps} = \begin{bmatrix} g_l\begin{pmatrix} g_p\bar{W}_{11}^2(\xi)\bar{W}_{11}^1(\xi) \\ +g_s\bar{W}_{12}^2(\xi)\bar{W}_{21}^1(\xi)\end{pmatrix} & g_l\begin{pmatrix} g_p\bar{W}_{11}^2(\xi)\bar{W}_{12}^1(\xi) \\ +g_s\bar{W}_{12}^2(\xi)\bar{W}_{22}^1(\xi)\end{pmatrix} \\ 1 & 0 \end{bmatrix}, \quad \bar{\boldsymbol{B}}_{lps} = \begin{bmatrix} g_l(g_p\bar{W}_{11}^2(\xi)\bar{W}_{13}^1(\xi) + g_s\bar{W}_{12}^2(\xi)\bar{W}_{23}^1(\xi)) \\ 0 \end{bmatrix}.$$

Similarly, these NN numerical models Eq. (51) could be transformed into the results as the following simulation LDI representation

$$\boldsymbol{x}(k+1) = \sum_{i=1}^{4} \bar{h}_i(k)(\bar{\boldsymbol{A}}_i\boldsymbol{x}(k) + \bar{\boldsymbol{B}}_i u(k)) \tag{52}$$

where

$$\begin{aligned}\bar{h}_1(k) &= \bar{h}_{11}^2(k)\bar{h}_{11}^1(k)\bar{h}_{21}^1(k) + \bar{h}_{11}^2(k)\bar{h}_{11}^1(k)\bar{h}_{22}^1(k) \\ &\quad +\bar{h}_{11}^2(k)\bar{h}_{12}^1(k)\bar{h}_{21}^1(k) + \bar{h}_{11}^2(k)\bar{h}_{12}^1(k)\bar{h}_{22}^1(k) \\ &\quad +\bar{h}_{12}^2(k)\bar{h}_{11}^1(k)\bar{h}_{21}^1(k), \\ \bar{h}_2(k) &= \bar{h}_{12}^2(k)\bar{h}_{11}^1(k)\bar{h}_{22}^1(k), \\ \bar{h}_3(k) &= \bar{h}_{12}^2(k)\bar{h}_{12}^1(k)\bar{h}_{21}^1(k), \\ \bar{h}_4(k) &= \bar{h}_{12}^2(k)\bar{h}_{12}^1(k)\bar{h}_{22}^1(k),\end{aligned}$$

and

$$\begin{aligned}&\bar{\boldsymbol{A}}_1 = \bar{\boldsymbol{A}}_{1ps} = \bar{\boldsymbol{A}}_{211}, \quad \bar{\boldsymbol{A}}_2 = \bar{\boldsymbol{A}}_{212}, \\ &\bar{\boldsymbol{A}}_3 = \bar{\boldsymbol{A}}_{221}, \quad \bar{\boldsymbol{A}}_4 = \bar{\boldsymbol{A}}_{222}, \\ &\bar{\boldsymbol{B}}_1 = \bar{\boldsymbol{B}}_{1ps} = \bar{\boldsymbol{B}}_{211}, \quad p,s = 1,2, \\ &\bar{\boldsymbol{B}}_2 = \bar{\boldsymbol{B}}_{212}, \quad \bar{\boldsymbol{B}}_3 = \bar{\boldsymbol{B}}_{221}, \quad \bar{\boldsymbol{B}}_4 = \bar{\boldsymbol{B}}_{222}.\end{aligned}$$

**Steps 7-8:** According to the LMI techniques (Tsai and Chen 2014), there exists a positive numerical definite matrix $\boldsymbol{Q}$ if the amplitude $\xi$ is within the interval 0.88-1.22 (see Fig. 6). That is to say, the simulation system Eq. (53) could be asymptotically and reasonably stabilized by the synthesized EBA fuzzy controller Eq. (40). Based on the backpropagation algorithm, the weights (with $\xi$ = 1.1) of the NN relaxed simulation system can be obtained as follows

$$\begin{aligned}&\bar{W}_{11}^1(1.1) = 1.0082, \quad \bar{W}_{12}^1(1.1) = 0.5019, \\ &\bar{W}_{13}^1(1.1) = 0.2171, \quad \bar{W}_{21}^1(1.1) = -0.1840, \\ &\bar{W}_{22}^1(1.1) = 0.8141, \quad \bar{W}_{23}^1(1.1) = -0.2381, \\ &\bar{W}_{31}^1(1.1) = -0.2354, \quad \bar{W}_{32}^1(0.9) = -1.1959.\end{aligned}$$

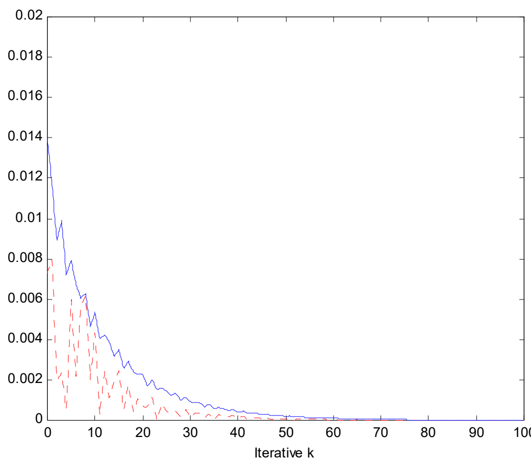


Fig. 6 The plots of bonding errors

Then, the matrices $\bar{\boldsymbol{A}}$ and $\bar{\boldsymbol{B}}$ are shown as below

$$\begin{aligned}&\bar{\boldsymbol{A}}_1 = \begin{bmatrix} 0 & 0 \\ 1 & 0 \end{bmatrix}, \quad \bar{\boldsymbol{A}}_2 = \begin{bmatrix} -0.0803 & 0.0043 \\ 1 & 0 \end{bmatrix}, \\ &\bar{\boldsymbol{A}}_3 = \begin{bmatrix} -0.2373 & -0.1181 \\ 1 & 0 \end{bmatrix}, \\ &\bar{\boldsymbol{A}}_4 = \begin{bmatrix} -0.0173 & -1.0917 \\ 1 & 0 \end{bmatrix}, \\ &\bar{\boldsymbol{B}}_1 = \begin{bmatrix} 0 \\ 0 \end{bmatrix}, \quad \bar{\boldsymbol{B}}_2 = \begin{bmatrix} 0.2847 \\ 0 \end{bmatrix}, \\ &\bar{\boldsymbol{B}}_3 = \begin{bmatrix} -0.0511 \\ 0 \end{bmatrix}, \quad \bar{\boldsymbol{B}}_4 = \begin{bmatrix} 0.2336 \\ 0 \end{bmatrix}.\end{aligned}$$

Next, the bounding matrix is chosen as

$$\bar{\boldsymbol{H}}_q = \begin{bmatrix} -0.0029 & -0.1073 \\ 0.12 & 0 \end{bmatrix}, \quad \delta_{ij} = I. \tag{53}$$

In accordance with the LMI techniques, we can obtain a positive definite matrix $\boldsymbol{Q}$ to satisfy Eq. (26)

$$\boldsymbol{Q} = \begin{bmatrix} 7.5807 & 2.1983 \\ 2.1983 & 6.0794 \end{bmatrix}.$$

Nevertheless, the proposed assumption of robustness design is satisfied and checked from the numerical illustration in Fig. 6. Thus, according to Theorem 4.1, the closed-loop simulation system (Eq. (42) + (40)) is asymptotically stable.

Like other swarm information algorithms and scalable mathematics methods, the EBA really requires optimal solution. Therefore, the same numerical experiment needs to be repeated in several times to check whether the mathematics convergence simulation results are all consistent. The medium used to transmit sound waves is air because it is suitable for the natural and real environment where bats are found. In addition, the overall size equals the number of people present in the resolution space at the same time in each iteration. The larger population size gives the algorithm a better chance of finding the nearest solution. However, there are a larger population needing more memory and even computing power. Therefore, in the numerical experiment, we reasonably set the population size to 16.

## 7. Conclusions

With neuron-based and fuzzy network- based mathematics methods of mathematics nonlinear simulation systems ensure that the design of the the smart algorithms is asymptotically stable in the study. First, we establish an NN model to numerically approximate the mathematics nonlinear numerical simulation system. These numerical dynamics of these NN numerical models are then changed to LDI representation. A robust design of a fuzzy controller based on neural network is proposed to solve the impact of modeling numerical error. These simulation results show that this method can make the mathematics nonlinear simulation system asymmetrically stable. These limitations of fuzzy logic and other AI techniques have led to further research on how to reduce the computations and improve the performance. A major breakthrough of this paper was the methodology of hybridization of combining artificial intelligence techniques by fuzzy theory, neural network and evolutional algorithm. The principle behind hybridization is to supplement the disadvantages with the advantages of the intelligent technology. The limitations of the proposed algorithm lack the practical applications. Therefore, the future study could be the synthesis and application of the novel developed AI hybridization into the practical engineering problems.

## References


Bedirhanoglu, I. (2014), "A practical neuro-fuzzy model for estimating modulus of elasticity of concrete", *Struct. Eng. Mech., Int. J.*, **51**(2), 249-265. https://doi.org/10.12989/sem.2014.51.2.249

Braz-Cesar, M.T. and Barros, R. (2018), "Semi-active fuzzy based control system for vibration reduction of a SDOF structure under seismic excitation", *Smart Struct. Syst., Int. J.*, **21**(4), 389-395. https://doi.org/10.12989/sss.2018.21.4.389

Chen, C.W. (2014a), "A criterion of robustness intelligent nonlinear control for multiple time-delay systems based on fuzzy Lyapunov methods", *Nonlinear Dyn.*, **76**(1), 23-31. https://doi.org/10.1007/s11071-013-0869-9

Chen, C.W. (2014b), "Interconnected TS fuzzy technique for nonlinear time-delay structural systems", *Nonlinear Dyn.*, **76**(1), 13-22. https://doi.org/10.1007/s11071-013-0841-8

Chen, T. (2020a), "LMI based criterion for reinforced concrete frame structures", *Adv. Concr. Constr., Int. J.*, **9**(4), 407-412. https://doi.org/10.12989/acc.2020.9.4.407

Chen, T. (2020b), "On the algorithmic stability of optimal control with derivative operators", *Circuits Syst. Signal Process*, **39**(12), 5863-5881. https://doi.org/10.1007/s00034-020- 01447-1

Chen, T. (2020c), "An intelligent algorithm optimum for building design of fuzzy structures", *Iran J. Sci. Technol, Trans Civil Eng.*, **44**, 523-531. https://doi.org/10.1007/s40996-019-00251-5

Chen, T. (2021), "Wind vibration control of stay cables using an evolutionary algorithm", *Wind Struct., Int. J.*, **32**(1), 73-86. https://doi.org/10.12989/was.2021.32.1.073

Chen, T. and Chen, C.Y.J. (2019), "Intelligent fuzzy algorithm for nonlinear discrete-time systems", *Transact. Inst. Measure. Control*, **42**(7), 1358-1374. https://doi.org/10.1177/0142331219891383

Chen, B.S., Tseng, C.S. and Uang, H.J. (1999), "R Robustness design of nonlinear dynamic systems via fuzzy linear control", *IEEE Trans. Fuzzy Syst.*, **7**(5), 571-585. https://doi.org/10.1109/91.797980

Chen, T., Khurram, S. and Cheng, C. (2019a), "A relaxed structural mechanics and fuzzy control for fluid–structure dynamic analysis", *Eng. Comput.*, **36**(7), 2200-2219. https://doi.org/10.1108/EC-11-2018-0522

Chen, T., Khurram, S. and Cheng, C. (2019b), "Prediction and control of buildings with sensor actuators of fuzzy EB algorithm", *Earthq. Struct., Int. J.*, **17**(3), 307-315. https://doi.org/10.12989/eas.2019.17.3.307

Chen, T., Babanin, A. Assim Muhammad, B. Chapron, Chen C.Y.J. (2020), "Evolved fuzzy NN control for discrete-time nonlinear systems", *J. Circuit. Syst. Comput.*, **29**(1), 2050015. https://doi.org/10.1142/S0218126620500152

Chen, T., Kuo, D. and Chen, C.Y.J. (2021), "Fuzzy C-means robust algorithm for nonlinear systems", *Soft Computing*, **25**(11), 7297-7305. https://doi.org/10.1007/s00500-021-05655-y

Desoer, C.A. and Shahruz, S.M. (1986), "Stability of dithered non-linear systems with backlash or hysteresis", *Int. J. Control*, **43**, 1045-1060. https://doi.org/10.1080/00207178608933522

Ghaffarzadeh, H. and Aghabalaei, K. (2017), "Adaptive fuzzy sliding mode control of seismically excited structures", *Smart Struct. Syst., Int. J.*, **19**(5), 577-585. https://doi.org/10.12989/sss.2017.19.5.577

Gutman, S. (1979), "Uncertain dynamic systems- a Lyapunov min-max approach", *IEEE Trans. Automatic Control*, **24**, 438-443. https://doi.org/10.1109/TAC.1979.1102073

Jeong, S., Lee, J., Cho, S. and Sim, S.H. (2019), "Integrated cable vibration control system using Arduino", *Smart Struct. Syst., Int. J.*, **23**(6), 695-702. https://doi.org/10.12989/sss.2019.23.6.695

Kirakidis, K. (1998), "Robust stabilization of the Takagi-Sugeno fuzzy model via bilinear matrix inequalities", *IEEE Transact. Fuzzy Syst.*, **9**(2), 269-277. https://doi.org/10.3397/1.3097762

Limanond, S. and Si, J. (1998), "Neural network-based control design: An LMI approach", *IEEE Trans. Neural Networks*, **9**(6), 1422-1429. https://doi.org/10.1109/72.728392

Pozo, F., Pujol, G. and Acho, L. (2016), "Vibration control of hysteretic base-isolated structures: an LMI approach", *Smart Struct. Syst., Int. J.*, **17**(2), 195-208. https://doi.org/10.12989/sss.2016.17.2.195

Safa, M., Shariati, M., Ibrahim, Z., Toghroli, A., Baharom, S.B., Nor, N.M. and Petkovic, D. (2016), "Potential of adaptive neuro fuzzy inference system for evaluating the factors affecting steel concrete composite beam's shear strength", *Steel Compos. Struct., Int. J.*, **21**(3), 679-688. https://doi.org/10.12989/scs.2016.21.3.679

Shariat, M., Shariati, M., Madadi, A. and Wakil, K. (2018), "Computational Lagrangian Multiplier Method by using optimization and sensitivity analysis of rectangular reinforced concrete beams", *Steel Compos. Struct., Int. J.*, **29**(2), 243-256. http://doi.org/10.12989/scs.2018.29.2.243

Shariatmadar, H. and Razavi, H.M. (2014), "Seismic control response of structures using an ATMD with fuzzy logic controller and PSO method", *Struct. Eng. Mech., Int. J.*, **51**(4), 547-564. https://doi.org/10.12989/sem.2014.51.4.547

Son, L., Bur, M., Rusli, M. and Adriyan, A. (2016), "Design of double dynamic vibration absorbers for reduction of two DOF vibration system", *Struct. Eng. Mech., Int. J.*, **57**(1), 161-178. https://doi.org/10.12989/sem.2016.57.1.161

Tanaka, K. (1995), "Stability and stabilizability of fuzzy-neural-linear control systems", *IEEE Trans. Fuzzy Syst.*, **3**(4), 438-447. https://doi.org/10.1109/91.481952

Tanaka, K. and Sugeno, M. (1992), "Stability analysis and design of fuzzy control systems", *Fuzzy Sets Syst.*, **45**(2), 135-156. https://doi.org/10.1016/0165-0114(92)90113-I

Tsai, P.W. and Chen, C.W. (2014), "A novel criterion for nonlinear time-delay systems using LMI fuzzy Lyapunov method", *Appl. Soft Comput.*, **25**, 461-472. https://doi.org/10.1016/j.asoc.2014.08.045

Tsai, P.W., Hayat, T., Ahmad, B. and Chen, C.W. (2015), "Structural system simulation and control via NN based fuzzy model", *Struct. Eng. Mech., Int. J.*, **56**(3), 385-407. https://doi.org/10.12989/sem.2015.56.3.385

Ying, Z.G., Ni, Y.Q. and Duan, Y.F. (2019), "Stochastic stability control analysis of an inclined stay cable under random and periodic support motion excitations", *Smart Struct. Syst., Int. J.*, **23**(6), 641-651. https://doi.org/10.12989/sss.2019.23.6.641

Zandi, Y., Shariati, M., Marto, A., Wei, X., Karaca, Z., Dao, D., Toghroli, A., Hashemi, M.H., Sedghi, Y., Wakil, K. and Khorami, M. (2018), "Computational investigation of the comparative analysis of cylindrical barns subjected to earthquake", *Steel Compos*. *Struct*., *Int*. *J*., **28**(4), 439-447. http://doi.org/10.12989/scs.2018.28.4.439

Zhang, Y. (2015), "A fuzzy residual strength based fatigue life prediction method", *Struct*. *Eng*. *Mech*., *Int*. *J*., **56**(2), 201-221. https://doi.org/10.12989/sem.2015.56.2.201

Zhou, X., Lin, Y. and Gu, M. (2015), "Optimization of multiple tuned mass dampers for large-span roof structures subjected to wind loads", *Wind Struct*., *Int*. *J*., **20**(3), 363-388. https://doi.org/10.12989/was.2015.20.3.363

*HJ*